**Vedran Mrzljak**
E-mail: vedran.mrzljak@riteh.hr
Faculty of Engineering, University of Rijeka, Vukovarska 58, 51000 Rijeka, Croatia
**Jan Kudláček**
E-mail: jan.kudlacek@fs.cvut.cz
Czech Technical University of Prague, Zikova 1903/4, 166 36 Prague 6, Czech Republic
**Sandi Baressi Šegota**
E-mail: sbaressisegota@riteh.hr
**Vedran Medica-Viola**
E-mail: vmedica@riteh.hr
Faculty of Engineering, University of Rijeka, Vukovarska 58, 51000 Rijeka, Croatia

# Energy and Exergy Analysis of Waste Heat Recovery Closed-Cycle Gas Turbine System while Operating with Different Mediums

## Abstract

In this paper is performed energy and exergy analysis of waste heat recovery closed-cycle gas turbine system. Analyzed system can use waste heat from various main propulsors (gas turbines or internal combustion engines). Basically, the observed system operates by using $CO_2$, what was the baseline for the analysis. It is investigated did the observed system, while retaining the same configuration, can operate with different operating mediums instead of $CO_2$. Other observed operating mediums were Air and Helium. During the change in operating medium, pressures and temperatures in some system operating points cannot remain the same as in the process with $CO_2$, but the intention was to perform only the necessary changes (to ensure proper operation of each system component). Obtained results show that the system, while retaining the same configuration, can operate by using different operating mediums. Energy analysis of the system shows that the whole configuration is composed to operate with $CO_2$, because the whole system energy efficiency is much higher than in operation with Air or Helium. The energy efficiency of the whole system during operation with $CO_2$ is 87.68%, with Air is 58.39% and operation with Helium gives energy efficiency of 49.25%. Exergy analysis of the observed system shows that the system has a good potential to operate with other mediums, because in any observed situation exergy efficiency of the whole system was higher than 50%. In this analysis the highest exergy efficiency of the whole system was obtained during operation with Air (57.76%). In the observed system, low-temperature regenerator and main turbo-compressor are detected as components which are highly influenced by the change of operating medium. Therefore, these two components should be a baseline for further improvements and system optimization.

**Keywords:** waste heat recovery, closed-cycle gas turbine, various operating mediums, energy analysis, exergy analysis

## 1. Introduction

One of the most important topics, in the field of marine engineering, is reducing harmful emissions from the ships and environmental protection [1-3]. Many researchers and scientists give a wide range of proposals how the required goals can be achieved [4, 5]. Also, it should be taken into account that the legislation in this field is each year, more and more rigorous [6, 7].

The most important goal in the ship emissions reducing is how exhaust gasses from the main propulsors can be effectively used [8]. As the main propulsors can be internal combustion engines (single fuel or dual-fuel) [9, 10], steam turbines [11, 12], gas turbines (and gas turbine combination with other propulsors) [13-15] or any other, there exist a wide range of temperatures and pressures available in the exhaust gases (as well as amount of heat) which can be used or transferred to another type of energy [16].

Many researchers agree that one of the possible solutions for effective usage of heat from exhaust gases (waste heat) is the application of closed-cycle gas turbines which transfer waste heat to electrical energy [17]. In the literature, there can be found several examples and the analyses of such systems [18, 19]. It should be highlighted that the dominant operating medium used in such systems, especially for the marine applications, is $CO_2$ [20-22]. Closed-cycle marine gas turbines which operates by using $CO_2$ are proved to be reliable, safe and adequately efficient, what means that the dominant part of waste heat can be transferred into the electrical energy [23].

In the land-based applications, closed-cycle gas turbine operation offers many benefits (along with several challenges) [24]. There are a lot of examples how closed-cycle gas turbine power plants can be effective and applicable in many regions and countries [25]. Therefore, there is no reason to believe that the closed-cycle gas turbine systems cannot be effective in marine applications in general, regardless of used operating medium.

The used techniques for the analysis of marine waste heat recovery closed-cycle gas turbine system in this paper are energy and exergy analyses. Both of the mentioned analyses are used in many research papers for the investigation of various power plants [26-28], a set of components from power plants [29, 30] or individual components [31-33]. The major advantage of these analyses is that they do not require any details about the component inner structure, they require only the knowledge of operating medium flows to and from each component (along with used or produced mechanical power) [34-36]. Such analyses are very useful in determining components which did not show good/acceptable performance and which should be improved (or replaced) [37, 38]. The final goal of such analyses is to present possibilities of any system to achieve its optimal performance.

From the literature review related to marine waste heat recovery closed-cycle gas turbine systems arises a few questions. Is the existing marine waste heat recovery closed-cycle gas turbine system capable for operation with any other medium instead of $CO_2$? Can the system configuration remain the same regardless of used operating

medium? Did the change in operating medium require significant change of pressure and temperature in all (or almost all) system operating points? Can other operating mediums result with better overall performance of the existing waste heat recovery closed-cycle gas turbine system?

The research presented in this paper offers answers to these questions. In this research is taken one existing waste heat recovery closed-cycle gas turbine system which basically operates by using $CO_2$. While retaining the same system configuration, it is investigated possibilities of implementing two other operating mediums (Air and Helium) instead of $CO_2$. It was analyzed which changes in operating medium temperatures and pressures should be performed throughout observed system (in comparison to operation with $CO_2$). For all the observed variants it is performed energy and exergy analyses of the whole system and each of its components. Obtained conclusions and results can be a guideline for future research and improvement of such systems.

## 2.    Description and operating characteristics of the analyzed waste heat recovery closed-cycle gas turbine system

Analyzed waste heat recovery closed-cycle gas turbine system is presented in Figure 1. Regardless of the operating medium using for its operation, the operating principle is always the same.

The Heat Recovery Heat Exchanger (HRHE) is a dominant heater in this system inside which operating medium is heated to the highest possible temperature by using exhaust gasses from the main marine propulsion system (gas turbine or internal combustion engine). Example of similar marine heat exchanger and its analysis can be found in [39].

Operating medium after HRHE has the highest possible temperature and is delivered to the gas turbine. The gas turbine is only mechanical power producer in the analyzed system and mechanical power is produced due to operating medium expansion through the turbine. The gas turbine is connected by the same shaft with both turbo-compressors (Main Turbo-Compressor – MTC and Recompression Turbo-Compressor – RTC) as well as with Electrical Generator (EG). A part of mechanical power produced in the gas turbine is used for the MTC and RTC drive (turbo-compressors are mechanical power consumers), while the remaining mechanical power produced in the turbine (useful power) is applied for the EG drive. The principle of mechanical power distribution is the same for closed-cycle and open-cycle gas turbines which drives any power consumer [40, 41].

After expansion in the turbine, operating medium still has a high enough temperature, which can be used somewhere in the process for the heating purposes. Therefore, after the turbine, operating medium passes through HTR (High-Temperature Regenerator) and LTR (Low-Temperature Regenerator) in which occurs heat transfer from hotter to colder operating medium, Figure 1.

After the heat transfer in HTR and LTR, operating medium with decreased temperature is delivered to flow splitter. The dominant part of operating medium mass flow rate from the flow splitter is delivered to cooler (in which occur additional cooling before compression in the MTC), while the remaining mass flow rate from the flow splitter is delivered directly to RTC (without additional cooling before RTC). In the cooler occurs heat transfer from main operating medium to cooling operating medium (it can be used any cooling operating medium).

MTC and RTC increase operating medium pressure and after both turbo-compressors operating medium has similar (almost identical) pressure. After pressure increase in the MTC, operating medium is heated in LTR and delivered to flow merger, while after the RTC operating medium is delivered directly to flow merger (without additional heating). Flow merger collects two operating medium streams (from both turbo-compressors) and cumulative operating medium mass flow rate after flow merger passes through HTR. It should be noted that all flow streams delivered to and released from the flow merger (operating points 9, 10 and 11 – Figure 1) have identical (or almost identical) temperatures and pressures, regardless of used operating medium. After additional heating in HTR, operating medium is delivered to HRHE and the whole process is continuously repeated.

The structure of waste heat recovery closed-cycle gas turbine system analyzed in this paper is presented in [42] where the operating medium was $CO_2$. In this paper will be analyzed can this process operate with some other operating medium instead of $CO_2$, without changing of process structure. It should be highlighted that introducing any other operating medium (instead of $CO_2$) will require changes of at least several temperatures in some operating points presented in Figure 1 (in comparison to process with $CO_2$). This change is required to ensure proper operation of each system component. Also, in this paper will not be investigated applicability of any other operating medium in the observed process in practice, but it should be highlighted that certain changes and modifications should be performed to allow operation of this process with any other operating medium. The aim of this paper is to investigate application possibility and consequences on the efficiencies and losses of each component and the whole system by using other operating mediums (instead of $CO_2$), without further research about modifications which should be applied in real application.

Also, it should be highlighted that the majority of operating mediums which can be used in the analyzed waste heat recovery closed-cycle gas turbine system requires additional tanks for adding or removing operating medium mass flow rate to or from the process presented in Figure 1. Along with tanks, additional compressors or turbo-compressors will also be necessary for the compression of operating medium on the pressure in flow splitter. Only if the Air is used as an operating medium, the additional tanks will not be required (Air will be taken directly from the atmosphere), but the additional compressor or turbo-compressor will still be required. Described additional subsystems were not analyzed in this paper.

Along with the presented, in the literature can be found examples of several other waste heat recovery closed-cycle gas turbine systems for marine applications [43, 44]. Its dominant function is in the most of the cases, additional mechanical power production from the exhaust gases.
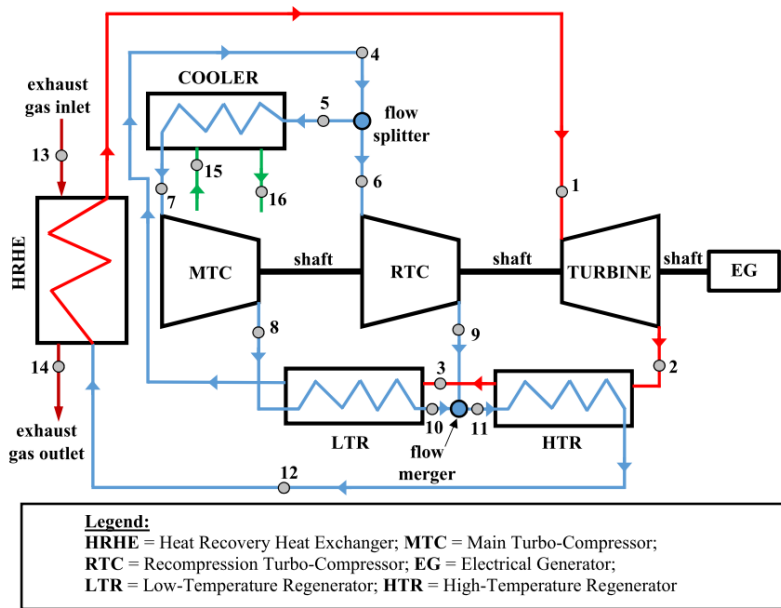


*Figure 1 - General scheme of the observed waste heat recovery closed-cycle gas turbine system along with operating points required for the analyses*

## 3. Equations for the energy and exergy analyses

### 3.1. General equations and balances

In the energy and exergy analyses of any system or a component, a few overall equations and balances must always be satisfied [45, 46]. The energy analysis is defined according to the first law of thermodynamics, which means that it is not dependable on the ambient conditions in which analyzed system or a component operates [47, 48]. As opposed to energy analysis, exergy analysis is defined according to the second law of thermodynamics and such analysis is notably influenced by the conditions of the ambient inside which observed system or a component operates [49, 50]. Therefore, in any exergy analysis a base ambient state (ambient temperature and pressure) for the calculations must be defined [51].

Overall energy and exergy balance equations, according to the literature [52-54] are:

$$\dot{Q}_{\text{in}} + P_{\text{in}} + \sum \dot{En}_{\text{in}} = \dot{Q}_{\text{out}} + P_{\text{out}} + \sum \dot{En}_{\text{out}}, \tag{1}$$

$$\dot{X}_{\text{h}} + P_{\text{in}} + \sum \dot{Ex}_{\text{in}} = P_{\text{out}} + \sum \dot{Ex}_{\text{out}} + \dot{Ex}_{\text{D}}. \tag{2}$$

Along with overall energy and exergy balance equations, general definition of energy or exergy efficiency, according to [55], can be presented by using an equation:

$$\eta_{\text{en (ex)}} = \frac{\text{cumulative energy (exergy) output}}{\text{cumulative energy (exergy) input}}. \tag{3}$$

It should be stated that Eq. 3 can be arranged much differently, regarding of operation characteristics and specifications of the system or a component [56, 57]. The fourth important general equation is mass flow rate balance [58]:

$$\sum \dot{m}_{\text{in}} = \sum \dot{m}_{\text{out}}. \tag{4}$$

In the most of the cases, in the energy or exergy analyses of any system or a component it is assumed that mass flow rate leakage of any operating medium stream did not occur. However, in the literature can also be found approaches which take into consideration mass flow rate leakage [59], especially in situations when leakage has an important influence on component operation.

In the equations above, $\dot{Q}$ is an energy transfer by heat, $P$ is mechanical power and $\dot{m}$ is operating medium mass flow rate. Furthermore, subscript in denotes input (inlet), subscript out denotes output (outlet), while subscript D denotes destruction (loss). $\dot{X}_{\text{h}}$ is an exergy transfer by heat at the temperature $T$, which can be calculated, according to literature [60], as:

$$\dot{X}_{\text{h}} = \sum (1 - \frac{T_0}{T}) \cdot \dot{Q}. \tag{5}$$

$\dot{En}$ is a total energy flow and $\dot{Ex}$ is a total exergy flow (both are related to any observed operating medium stream). Both of these variables are defined by the equations found in [61, 62]:

$$\dot{En} = \dot{m} \cdot h, \tag{6}$$

$$\dot{Ex} = \dot{m} \cdot \varepsilon. \tag{7}$$

In Eq. 6, $h$ is operating medium specific enthalpy, while $\varepsilon$ from Eq. 7 is operating medium specific exergy defined according to [63] as:

$$\varepsilon = (h - h_0) - T_0 \cdot (s - s_0). \tag{8}$$

In Eq. 8, $s$ is operating medium specific entropy while subscript 0 is related to the state of the ambient inside which observed system or a component operates. Eq. 2 and Eq. 8 proves that the ambient state notably influences the entire exergy analysis.

### 3.2. Equations for the calculation of energy and exergy destruction (loss) and efficiencies of each component and whole waste heat recovery system

In this subsection are presented equations for the energy and exergy destruction (loss) and efficiency calculation of the whole observed waste heat recovery closed-cycle gas turbine system and each of its components. It should be noted that all the equations shown in this subsection are valid for the observed system, regardless which operating medium is used. All the presented equations are based on the overall equations and balances from the previous subsection and on the recommendations from the literature [64-66].

In Table 1 are presented equations for the energy destruction (energy loss) and energy efficiency calculation of all heat exchangers from the observed system and it is explained how the same equations will be obtained in the exergy analysis. All the equations are based on the transmitted and received heat of each operating medium stream.

*Table 1 – Equations for the energy destruction (energy loss) and energy efficiency calculation of all heat exchangers from the observed waste heat recovery closed-cycle gas turbine system*

| Component* | Energy destruction** | Eq. | Energy efficiency** | Eq. |
|---|---|---|---|---|
| HRHE | $\dot{E}n_{D,HRHE} = \dot{E}n_{13} + \dot{E}n_{12} - \dot{E}n_{14} - \dot{E}n_1$ | (9) | $\eta_{en,HRHE} = \dfrac{\dot{E}n_1 - \dot{E}n_{12}}{\dot{E}n_{13} - \dot{E}n_{14}}$ | (12) |
| LTR | $\dot{E}n_{D,LTR} = \dot{E}n_3 + \dot{E}n_8 - \dot{E}n_{10} - \dot{E}n_4$ | (10) | $\eta_{en,LTR} = \dfrac{\dot{E}n_{10} - \dot{E}n_8}{\dot{E}n_3 - \dot{E}n_4}$ | (13) |
| HTR | $\dot{E}n_{D,HTR} = \dot{E}n_2 + \dot{E}n_{11} - \dot{E}n_{12} - \dot{E}n_3$ | (11) | $\eta_{en,HTR} = \dfrac{\dot{E}n_{12} - \dot{E}n_{11}}{\dot{E}n_2 - \dot{E}n_3}$ | (14) |

*\* Operating point numeration is performed according to markings from Figure 1.*

*\*\* Exergy destruction (exergy loss) and exergy efficiency for each heat exchanger are calculated while using the same equations, by replacing total energy flow ($\dot{E}n$) with the total exergy flow ($\dot{E}x$) of each operating medium stream and by replacing energy efficiency ($\eta_{en}$) with exergy efficiency ($\eta_{ex}$) of each heat exchanger.*

The observed system contains two turbo-compressors (MTC and RTC) which are mechanical power consumers as well as one gas turbine which is the mechanical power producer. Energy analysis of mechanical power producer and consumers is based on the comparison of its real (polytropic) and ideal (isentropic) compression and expansion processes, as presented in Figure 2, according to [67]. Mechanical power consumers consume more mechanical power during real compression processes (in comparison to the ideal ones), while turbine produces more mechanical power in the ideal expansion process (in comparison to the real one) [68]. Operating points in Figure 2 are in accordance to operating point markings from Figure 1. In the exergy analysis of MTC, RTC and gas turbine only the real (polytropic) compression and expansion processes are taken into consideration [69].
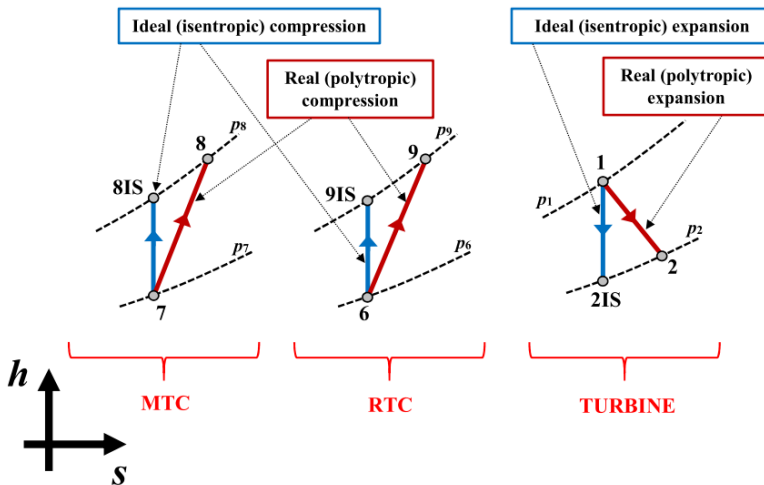


*Figure 2 - Specific enthalpy – specific entropy (h-s) diagrams for the energy analysis of MTC, RTC and TURBINE*

The equations for calculating used (turbo-compressors) and produced mechanical power (turbine) in ideal (isentropic) and real (polytropic) compression and expansion processes are presented in Table 2. Used and produced mechanical power (ideal and real) is also one of the essential elements for energy and exergy destructions (losses) and efficiency calculation of each turbo-compressor and turbine. Any mass flow rate leakage in the turbo-compressors or the turbine is neglected. Additionally, in Table 2 are presented equations for the calculation of useful mechanical power (in the ideal and real process).

*Table 2 - Equations for real (polytropic), ideal (isentropic) and useful mechanical power calculation*

| Component* | Mechanical power (real) | Eq. | Mechanical power (ideal) | Eq. |
|---|---|---|---|---|
| MTC | $P_{\text{MTC,re}} = \dot{m}_7 \cdot (h_8 - h_7)$ | (15) | $P_{\text{MTC,id}} = \dot{m}_7 \cdot (h_{8\text{IS}} - h_7)$ | (19) |
| RTC | $P_{\text{RTC,re}} = \dot{m}_6 \cdot (h_9 - h_6)$ | (16) | $P_{\text{RTC,id}} = \dot{m}_6 \cdot (h_{9\text{IS}} - h_6)$ | (20) |
| TURBINE | $P_{\text{TURB,re}} = \dot{m}_1 \cdot (h_1 - h_2)$ | (17) | $P_{\text{TURB,id}} = \dot{m}_1 \cdot (h_1 - h_{2\text{IS}})$ | (21) |
| USEFUL | $P_{\text{USEFUL,re}} = P_{\text{TURB,re}} - P_{\text{MTC,re}} - P_{\text{RTC,re}}$ | (18) | $P_{\text{USEFUL,id}} = P_{\text{TURB,id}} - P_{\text{MTC,id}} - P_{\text{RTC,id}}$ | (22) |

*\* Operating point numeration is performed according to markings from Figure 1 and Figure 2.*

Equations for the energy and exergy destruction (loss) and efficiency calculation of all turbo-compressors and the turbine from the observed system are presented in Table 3. All these equations presented in Table 3 are developed according to guidelines from the literature [70, 71].

*Table 3 - Equations for the energy and exergy destruction (loss) and efficiency calculation of all turbo-compressors and the turbine from the observed system*

| Component* | Energy destruction | Eq. | Energy efficiency | Eq. |
|---|---|---|---|---|
| MTC | $\dot{E}n_{\text{D,MTC}} = P_{\text{MTC,re}} - P_{\text{MTC,id}}$ | (23) | $\eta_{\text{en,MTC}} = \dfrac{P_{\text{MTC,id}}}{P_{\text{MTC,re}}}$ | (26) |
| RTC | $\dot{E}n_{\text{D,RTC}} = P_{\text{RTC,re}} - P_{\text{RTC,id}}$ | (24) | $\eta_{\text{en,RTC}} = \dfrac{P_{\text{RTC,id}}}{P_{\text{RTC,re}}}$ | (27) |
| TURBINE | $\dot{E}n_{\text{D,TURB}} = P_{\text{TURB,id}} - P_{\text{TURB,re}}$ | (25) | $\eta_{\text{en,TURB}} = \dfrac{P_{\text{TURB,re}}}{P_{\text{TURB,id}}}$ | (28) |
| Component* | Exergy destruction | Eq. | Exergy efficiency | Eq. |
| MTC | $\dot{E}x_{\text{D,MTC}} = \dot{E}x_7 + P_{\text{MTC,re}} - \dot{E}x_8$ | (29) | $\eta_{\text{ex,MTC}} = \dfrac{\dot{E}x_8 - \dot{E}x_7}{P_{\text{MTC,re}}}$ | (32) |
| RTC | $\dot{E}x_{\text{D,RTC}} = \dot{E}x_6 + P_{\text{RTC,re}} - \dot{E}x_9$ | (30) | $\eta_{\text{ex,RTC}} = \dfrac{\dot{E}x_9 - \dot{E}x_6}{P_{\text{RTC,re}}}$ | (33) |
| TURBINE | $\dot{E}x_{\text{D,TURB}} = \dot{E}x_1 - P_{\text{TURB,re}} - \dot{E}x_2$ | (31) | $\eta_{\text{ex,TURB}} = \dfrac{P_{\text{TURB,re}}}{\dot{E}x_1 - \dot{E}x_2}$ | (34) |

*\* Operating point numeration is performed according to markings from Figure 1 and Figure 2.*

Additionally, it should be stated that the equations for energy and exergy analyses of cooler in which the operating medium is cooled before compression in MTC are not presented. For the cooler is assumed always the same energy efficiency (equal to 98%), what is in accordance with the literature [72, 73], regardless of used operating medium (operating points 5 and 7, Figure 1) and regardless of used cooling medium (operating points 15 and 16, Figure 1).

For the flow splitter is assumed that the pressure and temperature of each operating medium stream at the splitter inlet and outlet are the same (the differences occur only in operating medium mass flow rates). The same assumption is also adopted for flow merger, Figure 1. Additionally, for the flow splitter is considered that 65% of inlet operating medium mass flow rate is delivered to the MTC (operating point 5, Figure 1), while 35% of inlet operating medium mass flow rate is delivered to the RTC (operating point 6, Figure 1). All mentioned assumptions related to flow splitter and flow merger are valid regardless of considered operating medium.

Calculation of energy and exergy destruction (loss) and efficiency for the whole observed system require definition of system boundaries. System boundaries of the whole system, presented in Figure 3, allows defining total energy and total exergy flow (Eq. 6 and Eq. 7) of each operating medium stream which enter and exit from the system.

For the whole observed system, inlet operating medium streams are exhaust gas at the HRHE inlet and cooling medium at the cooler inlet (operating points 13 and 15, Figure 1 and Figure 3), while outlet operating medium streams are exhaust gas at the HRHE outlet and cooling medium at the cooler outlet (operating points 14 and 16, Figure 1 and Figure 3). Additionally, outlet stream for the whole observed system is useful mechanical power, calculated by using Eq. 18.
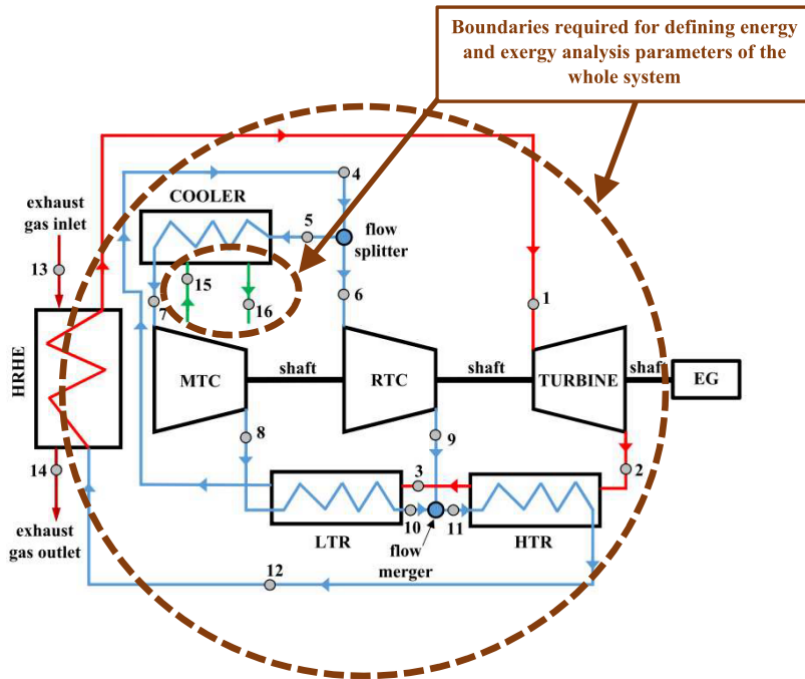
*Figure 3 - Boundaries required for the energy and exergy destruction (loss) and efficiency calculation of the whole observed system*

Equations for the energy destruction (energy loss) and energy efficiency calculation of the whole observed system are presented in Table 4. Also, under the Table 4 is explained how the same equations will be obtained for the whole system exergy analysis.

*Table 4 - Equations for the energy destruction (energy loss) and energy efficiency calculation of the whole observed waste heat recovery closed-cycle gas turbine system*

| - - - | Whole system (WS)** | Eq. |
|---|---|---|
| **Energy destruction*** | $$\dot{E}n_{\mathrm{D,WS}} = \dot{E}n_{13} + \dot{E}n_{15} - \dot{E}n_{14} - \dot{E}n_{16} - P_{\mathrm{USEFUL,re}}$$ | (35) |
| **Energy efficiency*** | $$\eta_{\mathrm{en,WS}} = \frac{P_{\mathrm{USEFUL,re}}}{\dot{E}n_{13} + \dot{E}n_{15} - \dot{E}n_{14} - \dot{E}n_{16}}$$ | (36) |

*\* Operating point numeration is performed according to markings from Figure 1.*

*\*\* Exergy destruction (exergy loss) and exergy efficiency for the whole system are calculated while using the same equations, by replacing total energy flow ($\dot{E}n$) with the total exergy flow ($\dot{E}x$) of each operating medium stream and by replacing energy efficiency ($\eta_{\mathrm{en}}$) with exergy efficiency ($\eta_{\mathrm{ex}}$).*

## 4. Thermodynamic parameters of waste heat recovery closed-cycle gas turbine system for every used operating medium

The configuration of analyzed system (Figure 1) and its main operating parameters (temperature, pressure and mass flow rate in each operating point from Figure 1) when the system operates with $CO_2$ are found in [42].

In this research the intention was to investigate did the closed-cycle gas turbine system of the same configuration can operate with other operating mediums instead of $CO_2$. There is no discussion that temperatures and/or pressures in several operating points from Figure 1 must be changed when any new operating medium is applied (to ensure proper operation of each component). However, the changes will be kept on the lowest possible level.

Therefore, it is mathematically investigated possibilities of the operating medium change, it is not investigated all the details and changes which will surely be required in practical implementation of some other operating medium.

Along with $CO_2$, two other selected operating mediums as a possible replacement in the analyzed system (while remaining the same system configuration) were Air and Helium. All three selected operating mediums are incorporated in NIST-REFPROP 9.0 software [74], which require two thermodynamic properties in each operating point to calculate all the others.

As stated before, in the energy analysis is not required definition of the ambient state in which observed system and its components operate, but such definition is essential in the exergy analysis [75]. Selected base ambient state for which are calculated specific exergies in each operating point from Figure 1, for each observed operating medium, is ambient pressure of 1 bar and ambient temperature of 25 °C. It should be noted that the base ambient state can be selected arbitrarily, but in this paper

it is selected according to recommendations from [76].

The general thermodynamic properties of observed operating mediums for the analyzed closed-cycle gas turbine system ($CO_2$, Air and Helium) is found in NIST-REFPROP 9.0 software and presented in Table 5.

*Table 5 – General thermodynamic properties of $CO_2$, Air and Helium used in this analysis*

| | | $CO_2$ | Air | Helium |
|---|---|---|---|---|
| **Molar mass (kg/kmol)** | | 44.01 | 28.965 | 4.0026 |
| **Triple point temperature (°C)** | | -56.558 | -213.4 | -270.97 |
| **Acentric factor (-)** | | 0.22394 | 0.0335 | -0.385 |
| **Critical point** | **Temperature (°C)** | 30.978 | -140.62 | -267.95 |
| | **Pressure (bar)** | 73.773 | 37.86 | 2.276 |
| | **Density (kg/m³)** | 467.6 | 342.68 | 72.567 |

Along with $CO_2$, Air and Helium, in the calculations were also used exhaust gases (for HRHE operation), and cooling mediums in cooler (water and nitrogen). General thermodynamic properties of all these mediums were not presented in this paper (it is presented properties only in operating points from Figure 1 related to these mediums), but it should be stated that all the required properties of all used mediums are incorporated in NIST-REFPROP 9.0 software and directly used for the calculations.

Properties of $CO_2$ in each operating point of the analyzed system are presented in Table 6 (base system). It should be noted that $CO_2$ mass flow rates, temperatures and pressures in each operating point are taken from [42], while specific enthalpies, specific entropies and specific exergies are calculated by using NIST-REFPROP 9.0 software. The same applies for exhaust gas and water.

*Table 6 - Properties of CO₂ in each operating point of the analyzed system\**

| O. P.** | Operating medium | Mass flow rate (kg/s) | Temperature (°C) | Pressure (bar) | Specific enthalpy (kJ/kg) | Specific entropy (kJ/kg·K) | Specific exergy (kJ/kg) |
|---|---|---|---|---|---|---|---|
| 1 | CO₂ | 57.00 | 435.00 | 174.70 | 896.27 | 2.5856 | 436.26 |
| 2 | CO₂ | 57.00 | 343.40 | 75.50 | 803.04 | 2.6026 | 337.94 |
| 3 | CO₂ | 57.00 | 184.40 | 74.70 | 623.97 | 2.2688 | 258.42 |
| 4 | CO₂ | 57.00 | 72.50 | 74.00 | 486.48 | 1.9236 | 223.84 |
| 5 | CO₂ | 37.05 | 72.50 | 74.00 | 486.48 | 1.9236 | 223.84 |
| 6 | CO₂ | 19.95 | 72.50 | 74.00 | 486.48 | 1.9236 | 223.84 |
| 7 | CO₂ | 37.05 | 29.98 | 72.10 | 304.38 | 1.3429 | 214.87 |
| 8 | CO₂ | 37.05 | 62.00 | 180.00 | 336.26 | 1.3901 | 232.69 |
| 9 | CO₂ | 19.95 | 158.90 | 178.20 | 546.80 | 1.9519 | 275.71 |
| 10 | CO₂ | 37.05 | 158.90 | 178.20 | 546.80 | 1.9519 | 275.71 |
| 11 | CO₂ | 57.00 | 158.90 | 178.20 | 546.80 | 1.9519 | 275.71 |
| 12 | CO₂ | 57.00 | 294.90 | 176.40 | 725.83 | 2.3155 | 346.34 |
| 13 | Exhaust gas | 54.70 | 490.00 | 1.01 | 908.08 | 4.8528 | 194.88 |
| 14 | Exhaust gas | 54.70 | 319.90 | 1.01 | 726.12 | 4.5832 | 93.28 |
| 15 | Water | 55.00 | 25.00 | 2.00 | 105.01 | 0.3672 | 0.10 |
| 16 | Water | 55.00 | 53.76 | 1.90 | 225.23 | 0.7521 | 5.54 |
|  |  |  |  |  |  |  |  |
| 2IS | CO₂ | 57.00 | 334.25 | 75.50 | 792.62 | 2.5856 | 332.60 |
| 8IS | CO₂ | 37.05 | 56.25 | 180.00 | 320.29 | 1.3429 | 231.08 |
| 9IS | CO₂ | 19.95 | 150.99 | 178.20 | 534.68 | 1.9236 | 272.03 |

*\* Properties of CO₂ are dominantly taken from [42]. Minor changes are applied to ensure an increase in specific entropy during compression and expansion processes. Ideal (isentropic) processes (operating points 2IS, 8IS and 9IS) are calculated by using NIST-REFPROP 9.0 software [74].*

*\*\* O. P. = Operating Point (in accordance with Figure 1 and Figure 3).*

During replacement of $CO_2$ with Air or Helium, several guidelines were followed:
- Exhaust gas mass flow rate, temperature and pressure at the HRHE inlet and outlet (operating points 13 and 14, Figure 1) remains always the same, regardless of the used operating medium in closed-cycle gas turbine system.
- Mass flow rates of Air and Helium at the HRHE inlet and outlet (operating points 12 and 1, Figure 1) were calculated by using HRHE energy and exergy balance equations. In other system operating points, Air and Helium mass flow

rates are calculated by following previously described procedure (Subsection 3.2.).

- In each operating point from Figure 1, pressures of the Air and Helium remains identical to $CO_2$ pressures.
- Temperatures of Air and Helium in several operating points from Figure 1 were changed (in comparison to $CO_2$ temperatures), to ensure proper operation of each component from the observed system.
- In the cooler, the selected cooling medium is Nitrogen with increased pressure (in comparison to water), when the closed-cycle operating medium was Air or Helium.
- Cooler energy efficiency remains always the same and equal to 98%.
- When the observed system operates with Air or Helium, specific enthalpies, specific entropies and specific exergies in each operating point are calculated using NIST-REFPROP 9.0 software.
- System configuration remains always the same.

The selection of Air and Helium as a replacement for $CO_2$ was not arbitrarily. According to the literature, both of selected operating mediums are good candidates which can commonly be used in closed-cycle gas turbine processes [77].

As stated before, in this paper is analyzed the main part of closed-cycle gas turbine system. The subsystem which involves operating medium tanks and compressors (or turbo-compressors) for delivering operating medium to (or from) the flow splitter is not analyzed. In the situation when Air is used as an operating medium in the closed-cycle gas turbine system, mentioned subsystem will have only compressor or turbo-compressor, additional tanks for operating medium will not be required because Air can be taken directly from the atmosphere. This fact can save space and make the presented system simpler than usual.

Helium has several advantages in comparison to other operating mediums commonly used for the operation of closed-cycle gas turbines [78]. Also, some land-based closed-cycle gas turbine power plants nowadays successfully operate by using Helium [79, 80]. As $CO_2$, Helium will also require additional tanks and compressors (or turbo-compressors) in the subsystem. Therefore, Helium is surely operating medium worth for consideration and $CO_2$ replacement in the observed system.

All finally obtained thermodynamic data in each operating point of the observed system when $CO_2$ is replaced with Air are presented in Table 7, while data of the observed system when it operate by using Helium are presented in Table 8.

*Table 7 - Properties of Air in each operating point of the analyzed system*

| O. P.* | Operating medium | Mass flow rate (kg/s) | Temperature (°C) | Pressure (bar) | Specific enthalpy (kJ/kg) | Specific entropy (kJ/kg·K) | Specific exergy (kJ/kg) |
|---|---|---|---|---|---|---|---|
| 1 | Air | 62.59 | 435.00 | 174.70 | 853.06 | 3.2800 | 608.80 |
| 2 | Air | 62.59 | 304.71 | 75.50 | 709.29 | 3.3080 | 456.66 |
| 3 | Air | 62.59 | 184.40 | 74.70 | 581.23 | 3.0627 | 401.74 |
| 4 | Air | 62.59 | 72.50 | 74.00 | 461.38 | 2.7649 | 370.68 |
| 5 | Air | 40.69 | 72.50 | 74.00 | 461.38 | 2.7649 | 370.68 |
| 6 | Air | 21.91 | 72.50 | 74.00 | 461.38 | 2.7649 | 370.68 |
| 7 | Air | 40.69 | -20.00 | 72.10 | 357.42 | 2.4215 | 369.12 |
| 8 | Air | 40.69 | 61.06 | 180.00 | 436.13 | 2.4300 | 445.28 |
| 9 | Air | 21.91 | 179.00 | 178.20 | 571.19 | 2.7798 | 476.04 |
| 10 | Air | 40.69 | 179.00 | 178.20 | 571.19 | 2.7798 | 476.04 |
| 11 | Air | 62.59 | 179.00 | 178.20 | 571.19 | 2.7798 | 476.04 |
| 12 | Air | 62.59 | 294.90 | 176.40 | 698.82 | 3.0343 | 527.79 |
| 13 | Exhaust gas | 54.70 | 490.00 | 1.01 | 908.08 | 4.8528 | 194.88 |
| 14 | Exhaust gas | 54.70 | 319.90 | 1.01 | 726.12 | 4.5832 | 93.28 |
| 15 | Nitrogen | 50.00 | -28.00 | 5.00 | 252.74 | 6.1533 | 147.98 |
| 16 | Nitrogen | 50.00 | 51.01 | 4.90 | 335.64 | 6.4524 | 141.69 |
|  |  |  |  |  |  |  |  |
| 2IS | Air | 62.59 | 289.76 | 75.50 | 693.31 | 3.2800 | 449.04 |
| 8IS | Air | 40.69 | 58.70 | 180.00 | 433.30 | 2.4215 | 444.99 |
| 9IS | Air | 21.91 | 172.96 | 178.20 | 564.48 | 2.7649 | 473.78 |

*\* O. P. = Operating Point (in accordance with Figure 1 and Figure 3).*

*Table 8 - Properties of Helium in each operating point of the analyzed system*

| O. P.* | Operating medium | Mass flow rate (kg/s) | Temperature (°C) | Pressure (bar) | Specific enthalpy (kJ/kg) | Specific entropy (kJ/kg·K) | Specific exergy (kJ/kg) |
|---|---|---|---|---|---|---|---|
| 1 | Helium | 9.55 | 435.00 | 174.70 | 3735.10 | 21.8120 | 4036.40 |
| 2 | Helium | 9.55 | 254.32 | 75.50 | 2767.78 | 22.0200 | 3007.00 |
| 3 | Helium | 9.55 | 207.00 | 74.70 | 2521.90 | 21.5540 | 2900.00 |
| 4 | Helium | 9.55 | 55.00 | 74.00 | 1732.60 | 19.5980 | 2694.10 |
| 5 | Helium | 6.21 | 55.00 | 74.00 | 1732.60 | 19.5980 | 2694.10 |
| 6 | Helium | 3.34 | 55.00 | 74.00 | 1732.60 | 19.5980 | 2694.10 |
| 7 | Helium | 6.21 | -50.00 | 72.10 | 1186.30 | 17.6470 | 2729.30 |
| 8 | Helium | 6.21 | 50.00 | 180.00 | 1740.00 | 17.6810 | 3272.90 |
| 9 | Helium | 3.34 | 195.00 | 178.20 | 2491.70 | 19.6250 | 3445.10 |
| 10 | Helium | 6.21 | 195.00 | 178.20 | 2491.70 | 19.6250 | 3445.10 |
| 11 | Helium | 9.55 | 195.00 | 178.20 | 2491.70 | 19.6250 | 3445.10 |
| 12 | Helium | 9.55 | 240.00 | 176.40 | 2724.50 | 20.1220 | 3529.70 |
| 13 | Exhaust gas | 54.70 | 490.00 | 1.01 | 908.08 | 4.8528 | 194.88 |
| 14 | Exhaust gas | 54.70 | 319.90 | 1.01 | 726.12 | 4.5832 | 93.28 |
| 15 | Nitrogen | 35.00 | -60.00 | 5.00 | 218.98 | 6.0057 | 158.22 |
| 16 | Nitrogen | 35.00 | 30.32 | 4.90 | 313.97 | 6.3833 | 140.62 |
| | | | | | | | |
| 2IS | Helium | 9.55 | 233.62 | 75.50 | 2660.3 | 21.812 | 2961.50 |
| 8IS | Helium | 6.21 | 47.91 | 180.00 | 1729.1 | 17.647 | 3272.10 |
| 9IS | Helium | 3.34 | 192.59 | 178.20 | 2479.3 | 19.598 | 3440.60 |

*\* O. P. = Operating Point (in accordance with Figure 1 and Figure 3).*

## 5. Results and discussion

Real (polytropic) mechanical power developed by the turbine, used by MTC and RTC, and finally useful mechanical power of the whole system for all three observed operating mediums ($CO_2$, Air and Helium) are presented in Figure 4.

Developed mechanical power by a turbine, using operating parameters presented in Table 6, Table 7 and Table 8 will be the highest if the observed system operates with Helium, while $CO_2$ as an operating medium gives the lowest mechanical power developed by the turbine. Air as an operating medium resulted with developed mechanical power slightly lower than in situation when the Helium is used, but significantly higher in comparison to $CO_2$.

Both turbo-compressors (MTC as well as RTC) consumes much higher mechanical power if the operating medium is Air or Helium (in comparison to $CO_2$). The highest mechanical power consumption of both turbo-compressors occurs if the Helium is used.

Useful mechanical power, which will be applied for the EG drive is the highest when the observed system operates with Air (3391.38 kW). Using a Helium as an operating medium results with useful mechanical power equal to 3264.67 kW, while the useful mechanical power will be the lowest when the observed system operates with $CO_2$.

It can be concluded that if the observed system use Air or Helium instead of $CO_2$, the result will be a notable increase of both produced and consumed mechanical power, what will finally lead to very similar useful mechanical power for the EG drive (as in the situation when $CO_2$ is used).
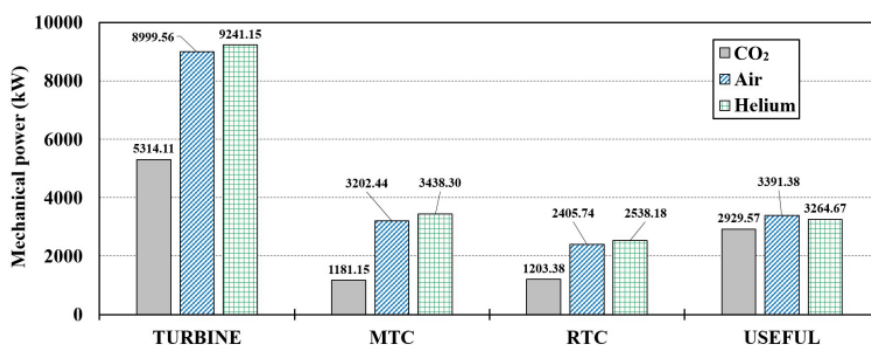


*Figure 4 - Developed (TURBINE), used (MTC and RTC) and useful mechanical power of the system for three observed operating mediums*

Energy destruction (energy loss) of all the components, as well as of the whole observed system during operation with each of three observed operating mediums is presented in Figure 5.

HRHE has the lowest energy destruction during operation with $CO_2$, while operation with Air and Helium result with identical energy destructions, which are higher than in operation with $CO_2$. HTR has the lowest energy destruction during operation with $CO_2$ and the highest energy destruction during operation with Helium.

When observing energy destruction of both turbo-compressors (MTC and RTC), the highest energy destruction can be observed in operation with $CO_2$ and the lowest energy destruction can be seen during operation with Helium. Energy destruction of the turbine increases while replacing $CO_2$ with Air or Helium (the highest energy destruction of the turbine can be noted during operation with Helium).

Energy destruction of a LTR and the whole system notably increase by replacing $CO_2$ with Air, while replacing $CO_2$ with Helium result with an even higher increase

in energy destruction of a LTR and WS (in comparison to Air). Therefore, it is clear that LTR is the component which is dominantly influenced with operating medium replacement.

From Figure 5 can be finally concluded that replacement of $CO_2$ with Air or Helium increases energy destruction of all heat exchangers (the dominant change can be seen in a LTR), of the turbine, as well as of the whole system. Both turbo-compressors will operate with lower energy destruction during such replacement. Furthermore, replacement of operating medium in the observed system, without the change of its structure, will increase overall system energy destruction (energy loss). Comparison of operation with Air and Helium shows notably higher energy destruction of the whole system during operation with Helium.
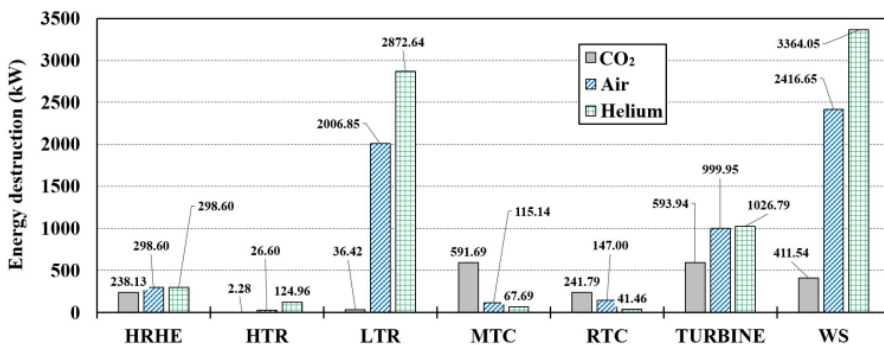


*Figure 5 – Energy destructions (energy losses) of the components and the whole system for three observed operating mediums*

In the scientific and professional literature can be found a general conclusion that energy destruction and energy efficiency of a system and its components are reverse proportional [81, 82]. The same conclusion is also valid for the system analyzed in this paper when considering all three operating mediums. The only component which deviates from mentioned general conclusion is gas turbine which energy efficiency remains almost identical (around 90%), regardless of used operating medium, Figure 6. For the same component (gas turbine), from Figure 5 can be seen that energy destruction strongly differs, what depends on the selected operating medium.

Energy efficiency of HRHE, for all observed operating mediums, is around 97% (the highest HRHE energy efficiency of 97.61% can be observed when the system operates with $CO_2$). HTR has energy efficiency very close to 100% when the system operates with $CO_2$ and Air, while HTR energy efficiency is slightly lower (94.68%) when the system operates with Helium.

Energy efficiency of LTR notably decreases when $CO_2$ is replaced with Air (from 99.54% to 73.25%) and even higher decrease in LTR energy efficiency occurs during

$CO_2$ replacement with Helium (from 99.54% to 61.90%). Both energy destruction and efficiency shows degradation of LTR performance when $CO_2$ is replaced with Air or Helium.

The energy efficiency of both turbo-compressors (MTC and RTC) increases when the system uses Air instead of $CO_2$, while using Helium gives even higher energy efficiencies of both turbo-compressors. It should be noted that MTC has a very low energy efficiency during operation with $CO_2$, what can be a result of inaccuracies during measurements of temperature and pressure, or can be a reason for MTC maintenance (and possible replacement) in a short time period.

Energy efficiency of whole observed system shows that the best performance (system energy efficiency of 87.68%) is obtained when the system uses $CO_2$ as operating medium. This is an expected fact, because this system is basically constructed to operate with $CO_2$. A change of operating medium results with a decrease in whole system energy efficiency, which is equal to 58.39% when the operating medium is Air and 49.25% when the operating medium is Helium.
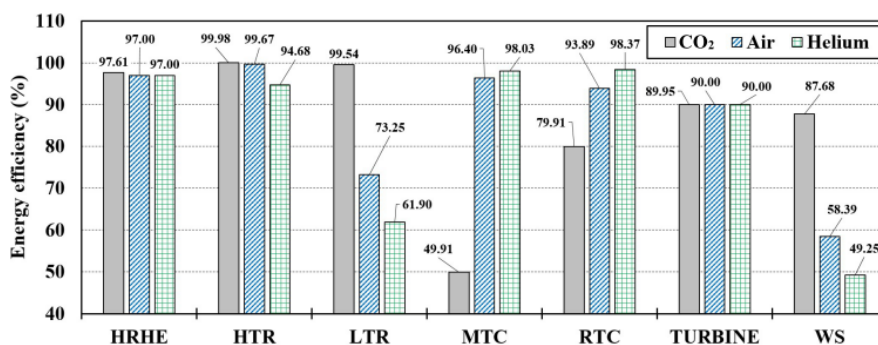


*Figure 6 – Energy efficiencies of the components and the whole system for three observed operating mediums*

Exergy destructions of the whole observed system and all of its components for three analyzed operating mediums are presented in Figure 7.

From Figure 7 can be concluded that change in operating medium has the same trend for HRHE, LTR, turbine and the whole system – exergy destructions of mentioned components and the whole system increases during operating medium change. For all the mentioned components and the whole system, exergy destructions are higher for Air (in comparison to $CO_2$), while for Helium is visible further increase in exergy destructions (in comparison to Air).

HTR exergy destruction decreases if $CO_2$ is replaced with Air or Helium. Also, for HTR is valid that the lowest exergy destruction is obtained during the operation with Air.

Both turbo-compressors (MTC and RTC) show the same trend when $CO_2$ is replaced with Air and Helium. MTC and RTC have the highest exergy destruction when operating with $CO_2$. Replacing of $CO_2$ with Air reduces exergy destructions of both turbo-compressors, while replacing $CO_2$ with Helium will result with the lowest exergy destructions of both turbo-compressors.

Comparison of Figure 5 and Figure 7 (comparison of energy and exergy destructions) shows the same trend for almost all the components and for the whole system during operating medium replacement. HTR is the only component which did not follow the same trend during operating medium replacement (HTR energy destruction is the lowest, but exergy destruction is the highest during operation with $CO_2$).
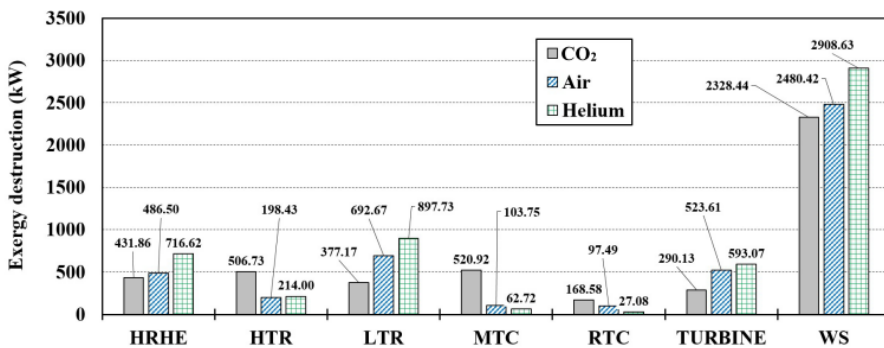


*Figure 7 – Exergy destructions (exergy losses) of the components and the whole system for three observed operating mediums*

Exergy efficiencies of the components and the whole analyzed system for three observed operating mediums are presented in Figure 8. As in energy analysis, in exergy analysis is also valid general conclusion that exergy destruction and exergy efficiency are reverse proportional. This fact is proved for the most of the components, but the same conclusion is not valid for the whole system. The whole system exergy destruction is the lowest when the system operates by using $CO_2$ (Figure 7), but the highest exergy efficiency of the whole system is obtained during the operation with Air (57.76%, Figure 8). The whole system has the highest exergy destruction during operation with Helium as well as the lowest exergy efficiency of 52.88%. In base operation with $CO_2$, the whole system has exergy efficiency equal to 55.72%. Regardless of used operating medium, it can be stated that exergy efficiency of the analyzed waste heat recovery closed-cycle gas turbine system is high enough for practical implementation.

Operating medium replacement from $CO_2$ to Air and finally to Helium results with a continuous decrease in exergy efficiency of HRHE, LTR and gas turbine, while the same replacement resulted with continuous increase in exergy efficiency of both

turbo-compressors, Figure 8. HTR has the highest exergy efficiency when the system operates by using Air (94.23%).

From Figure 8 can be concluded that the LTR operation by using Helium and MTC operation by using $CO_2$ resulted with a low exergy efficiency of both components, therefore the performance optimization (for LTR) and maintenance or replacing (for MTC) are obviously required.

In comparison to energy analysis, many components of the observed system show the same trends also in exergy analysis, but the most important conclusion from the exergy analysis is that the presented system (Figure 1) can adequately operate with other operating mediums (not only with $CO_2$). As the energy analysis, exergy analysis also shows several components which performance should be improved to obtain optimal operation.
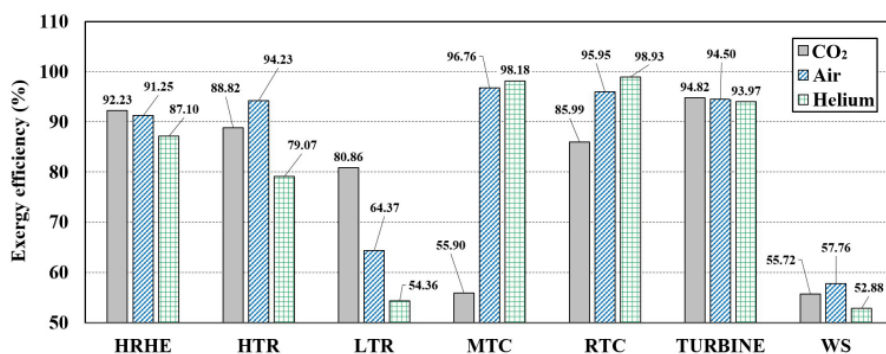


*Figure 8 – Exergy efficiencies of the components and the whole system for three observed operating mediums*

Further research of the presented and analyzed system can and will be performed in several different ways. Firstly, it will be investigated improvement possibilities for each system component when the system configuration remains the same (as presented in Figure 1). After that, it will be investigated different system configurations with an aim to find an optimal one for each operating medium. All of newly obtained system configurations will be optimized by using various conventional [83, 84] and artificial intelligence methods and techniques, which show its potential not only in marine applications [85, 86], but also in energy systems [87], medical applications [88, 89], robotics [90], in predicting trends of global (or local) diseases [91-93], etc.

## 6. Conclusions

This paper presents energy and exergy analyses of waste heat recovery closed-cycle gas turbine system while running by using different operating mediums. The base operating medium was $CO_2$, while the additionally investigated was Air and Helium. The main goal was to retain system configuration and perform as small as possible change of pressure and temperature in certain system operating points during the change in operating medium. Analysis of the whole system and all of its constituent components, while running on different operating mediums, lead to several interesting conclusions:

- It is possible to change closed-cycle gas turbine operating medium while retaining the same system configuration and with minor changes of temperatures in a certain operating points (to ensure proper operation of each component).
- Energy analysis of the whole system shows that the system is designed to operate by using $CO_2$, because in that situation its energy efficiency is the highest (equal to 87.68%). The operating medium change resulted with significant decrease of whole system energy efficiency.
- Exergy analysis of the whole system shows that all of the observed operating mediums ($CO_2$, Air, Helium) can be a good candidates for a system operation because obtained exergy efficiency of the whole system, regardless of used operating medium, is higher than 50%. The highest system exergy efficiency is obtained by using the Air (57.76%).
- During the change in operating medium, low-temperature regenerator (LTR) is a component which efficiencies (both energy and exergy) notably decrease, so this component should be a baseline for the future improvements.
- Main turbo-compressor (MTC) is a component which operates with very low efficiencies in a base system (while using $CO_2$). Therefore, this component in the presented system requires improvement or reparation. Operation with other operating mediums show that the improvement potential of MTC is significant.

Finally, it should be highlighted once again that operating medium change of waste heat recovery closed-cycle gas turbine system will surely require several changes and minor modifications of the system in practical implementation. The practical implementation of the operating medium change is not investigated in this paper, but it is proved that in such system a different operating medium can be introduced without significant system modifications (while retaining the system configuration).

## Acknowledgment

## References

1.  Lion, S., Vlaskos, I., & Taccani, R. (2020). A review of emissions reduction technologies for low and medium speed marine Diesel engines and their potential for waste heat recovery. Energy Conversion and Management, 207, 112553. (doi:10.1016/j.enconman.2020.112553)
2.  Witkowski, K. (2020). Research of the effectiveness of selected methods of reducing toxic exhaust emissions of marine diesel engines. Journal of Marine Science and Engineering, 8(6), 452. (doi:10.3390/jmse8060452)
3.  Winnes, H., Fridell, E., & Moldanová, J. (2020). Effects of marine exhaust gas scrubbers on gas and particle emissions. Journal of Marine Science and Engineering, 8(4), 299. (doi:10.3390/jmse8040299)
4.  Yang, Z. L., Zhang, D., Caglayan, O., Jenkinson, I. D., Bonsall, S., Wang, J., ... & Yan, X. P. (2012). Selection of techniques for reducing shipping NOx and SOx emissions. Transportation Research Part D: Transport and Environment, 17(6), 478-486. (doi:10.1016/j.trd.2012.05.010)
5.  Muše, A., Jurić, Z., Račić, N., & Radica, G. (2020). Modelling, performance improvement and emission reduction of large two-stroke diesel engine using multi-zone combustion model. Journal of Thermal Analysis and Calorimetry, 1-14. (doi:10.1007/s10973-020-09321-7)
6.  Van, T. C., Ramirez, J., Rainey, T., Ristovski, Z., & Brown, R. J. (2019). Global impacts of recent IMO regulations on marine fuel oil refining processes and ship emissions. Transportation Research Part D: Transport and Environment, 70, 123-134.(doi:10.1016/j.trd.2019.04.001)
7.  Ni, P., Wang, X., & Li, H. (2020). A review on regulations, current status, effects and reduction strategies of emissions for marine diesel engines. Fuel, 279, 118477. (doi:10.1016/j.fuel.2020.118477)
8.  Kyriakidis, F., Sørensen, K., Singh, S., & Condra, T. (2017). Modeling and optimization of integrated exhaust gas recirculation and multi-stage waste heat recovery in marine engines. Energy Conversion and Management, 151, 286-295. (doi:10.1016/j.enconman.2017.09.004)
9.  Senčić, T., Mrzljak, V., Blecich, P., & Bonefačić, I. (2019). 2D CFD simulation of water injection strategies in a large marine engine. Journal of Marine Science and Engineering, 7(9), 296. (doi:10.3390/jmse7090296)
10. Tian, Z., Yue, Y., Gu, B., Gao, W., & Zhang, Y. (2020). Thermo-economic analysis and optimization of a combined Organic Rankine Cycle (ORC) system with LNG cold energy and waste heat recovery of dual-fuel marine engine. International Journal of Energy Research, 44(13), 9974-9994. (doi:10.1002/er.5529)
11. Mrzljak, V., Poljak, I., & Medica-Viola, V. (2017). Dual fuel consumption and efficiency of marine steam generators for the propulsion of LNG carrier. Applied Thermal Engineering, 119, 331-346. (doi:10.1016/j.applthermaleng.2017.03.078)
12. Koroglu, T., & Sogut, O. S. (2018). Conventional and advanced exergy analyses of a marine steam power plant. Energy, 163, 392-403. (doi:10.1016/j.energy.2018.08.119)
13. Bai, M., Liu, J., Ma, Y., Zhao, X., Long, Z., & Yu, D. (2021). Long short-term memory network-based normal pattern group for fault detection of three-shaft marine gas turbine. Energies, 14(1), 13. (doi:10.3390/en14010013)
14. Lorencin, I., Anđelić, N., Mrzljak, V., & Car, Z. (2019). Multilayer perceptron approach to condition-based maintenance of marine CODLAG propulsion system components. Pomorstvo, 33(2), 181-190. (doi:10.31217/p.33.2.8)
15. Anđelić, N., Baressi Šegota, S., Lorencin, I., & Car, Z. (2020). Estimation of gas turbine shaft torque and fuel flow of a CODLAG propulsion system using genetic programming algorithm. Pomorstvo, 34(2), 323-337. (doi:10.31217/p.34.2.13)
16. Singh, D. V., & Pedersen, E. (2016). A review of waste heat recovery technologies for maritime applications. Energy conversion and management, 111, 315-328. (doi:10.1016/j.enconman.2015.12.073)

17. Zare, V. (2020). Performance improvement of biomass-fueled closed cycle gas turbine via compressor inlet cooling using absorption refrigeration; thermoeconomic analysis and multi-objective optimization. Energy Conversion and Management, 215, 112946. (doi:10.1016/j.enconman.2020.112946)

18. Jackson, A. J., Codeceira Neto, A., Whellens, M. W., & Audus, H. (2000, May). Gas turbine performance using carbon dioxide as working fluid in closed cycle operation. In Turbo Expo: Power for Land, Sea, and Air (Vol. 78552, p. V002T04A005). American Society of Mechanical Engineers. (doi:10.1115/2000-GT-0153)

19. Kunniyoor, V., Singh, P., & Nadella, K. (2020). Value of closed-cycle gas turbines with design assessment. Applied Energy, 269, 114950. (doi:10.1016/j.apenergy.2020.114950)

20. Sharma, O. P., Kaushik, S. C., & Manjunath, K. (2017). Thermodynamic analysis and optimization of a supercritical CO2 regenerative recompression Brayton cycle coupled with a marine gas turbine for shipboard waste heat recovery. Thermal Science and Engineering Progress, 3, 62-74. (doi:10.1016/j.tsep.2017.06.004)

21. Manjunath, K., Sharma, O. P., Tyagi, S. K., & Kaushik, S. C. (2018). Thermodynamic analysis of a supercritical/transcritical CO2 based waste heat recovery cycle for shipboard power and cooling applications. Energy Conversion and Management, 155, 262-275. (doi:10.1016/j.enconman.2017.10.097)

22. Manente, G., & Fortuna, F. M. (2019). Supercritical CO2 power cycles for waste heat recovery: A systematic comparison between traditional and novel layouts with dual expansion. Energy Conversion and Management, 197, 111777. (doi:10.1016/j.enconman.2019.111777)

23. Mrzljak, V., Poljak, I., Prpić-Oršić, J., & Jelić, M. (2020). Exergy analysis of marine waste heat recovery CO2 closed-cycle gas turbine system. Pomorstvo, 34(2), 309-322. (doi:10.31217/p.34.2.12)

24. Olumayegun, O., Wang, M., & Kelsall, G. (2016). Closed-cycle gas turbine for power generation: A state-of-the-art review. Fuel, 180, 694-717. (doi:10.1016/j.fuel.2016.04.074)

25. McDonald, C. F. (2012). Helium turbomachinery operating experience from gas turbine power plants and test facilities. Applied Thermal Engineering, 44, 108-142. (doi:10.1016/j.applthermaleng.2012.02.041)

26. Adibhatla, S., & Kaushik, S. C. (2014). Energy and exergy analysis of a super critical thermal power plant at various load conditions under constant and pure sliding pressure operation. Applied thermal engineering, 73(1), 51-65. (doi:10.1016/j.applthermaleng.2014.07.030)

27. Ahmadi, G. R., & Toghraie, D. (2016). Energy and exergy analysis of Montazeri steam power plant in Iran. Renewable and Sustainable Energy Reviews, 56, 454-463. (doi:10.1016/j.rser.2015.11.074)

28. Aliyu, M., AlQudaihi, A. B., Said, S. A., & Habib, M. A. (2020). Energy, exergy and parametric analysis of a combined cycle power plant. Thermal Science and Engineering Progress, 15, 100450. (doi:10.1016/j.tsep.2019.100450)

29. Nandini, M., Sekhar, Y. R., & Subramanyam, G. (2021). Energy analysis and water conservation measures by water audit at thermal power stations. Sustainable Water Resources Management, 7(1), 1-24. (doi:10.1007/s40899-020-00487-4)

30. Chopra, K., Tyagi, V. V., Pandey, A. K., Ma, Z., & Ren, H. (2021). Energy, exergy, enviroeconomic & exergoeconomic (4E) assessment of thermal energy storage assisted solar water heating system: Experimental & theoretical approach. Journal of Energy Storage, 35, 102232. (doi:10.1016/j.est.2021.102232)

31. Anđelić, N., Mrzljak, V., Lorencin, I., & Baressi Šegota, S. (2020). Comparison of Exergy and Various Energy Analysis Methods for a Main Marine Steam Turbine at Different Loads. Pomorski zbornik, 59(1), 9-34. (doi:10.18048/2020.59.01.)

32. Mrzljak, V., Blecich, P., Anđelić, N., & Lorencin, I. (2019). Energy and exergy analyses of forced draft fan for marine steam propulsion system during load change. Journal of Marine Science and Engineering, 7(11), 381. (doi:10.3390/jmse7110381)

33. Medica-Viola, V., Baressi Šegota, S., Mrzljak, V., & Štifanić, D. (2020). Comparison of conventional and heat balance based energy analyses of steam turbine. Pomorstvo, 34(1), 74-85. (doi:10.31217/p.34.1.9)

34. Fadhil, A. N., Shihab, A. P. A. S., & Faisal, S. H. (2017). Assessment of AL-Hartha Steam Power Station Using Energy and Exergy Analysis. International Journal of Modern Studies in Mechanical Engineering, 3(2), 17-30. (doi:10.20431/2454-9711.0302003)

35. Baressi Šegota, S., Lorencin, I., Anđelić, N., Mrzljak, V., & Car, Z. (2020). Improvement of Marine

Steam Turbine Conventional Exergy Analysis by Neural Network Application. Journal of Marine Science and Engineering, 8(11), 884. (doi:10.3390/jmse8110884)

36. Mrzljak, V., Poljak, I., & Medica-Viola, V. (2017). Energy and exergy efficiency analysis of sealing steam condenser in propulsion system of LNG carrier. NAŠE MORE: znanstveni časopis za more i pomorstvo, 64(1), 20-25. (doi:10.17818/NM/2017/1.4)

37. Marais, H., Van Schoor, G., & Uren, K. R. (2019). The merits of exergy-based fault detection in petrochemical processes. Journal of Process Control, 74, 110-119. (doi:10.1016/j.jprocont.2017.11.005)

38. Njoku, H. O., Egbuhuzor, L. C., Eke, M. N., Enibe, S. O., & Akinlabi, E. A. (2019). Combined pinch and exergy evaluation for fault analysis in a steam power plant heat exchanger network. Journal of Energy Resources Technology, 141(12). (doi:10.1115/1.4043746)

39. Mrzljak, V., Poljak, I., & Medica-Viola, V. (2017). Thermodynamical analysis of high-pressure feed water heater in steam propulsion system during exploitation. Brodogradnja: Teorija i praksa brodogradnje i pomorske tehnike, 68(2), 45-61. (doi:10.21278/brod68204)

40. Liu, Z., & Karimi, I. A. (2020). Gas turbine performance prediction via machine learning. Energy, 192, 116627. (doi:10.1016/j.energy.2019.116627)

41. Mrzljak, V., Anđelić, N., Lorencin, I., & Car, Z. (2019). Analysis of gas turbine operation before and after major maintenance. Pomorski zbornik, 57(1), 57-70. (doi:10.18048/2019.57.04.)

42. Zhang, Q., Ogren, R. M., & Kong, S. C. (2018). Thermo-economic analysis and multi-objective optimization of a novel waste heat recovery system with a transcritical CO2 cycle for offshore gas turbine application. Energy conversion and management, 172, 212-227. (doi:10.1016/j.enconman.2018.07.019)

43. Feng, Y., Du, Z., Shreka, M., Zhu, Y., Zhou, S., & Zhang, W. (2020). Thermodynamic analysis and performance optimization of the supercritical carbon dioxide Brayton cycle combined with the Kalina cycle for waste heat recovery from a marine low-speed diesel engine. Energy Conversion and Management, 206, 112483. (doi:10.1016/j.enconman.2020.112483)

44. Hou, S., Wu, Y., Zhou, Y., & Yu, L. (2017). Performance analysis of the combined supercritical CO2 recompression and regenerative cycle used in waste heat recovery of marine gas turbine. Energy Conversion and Management, 151, 73-85. (doi:10.1016/j.enconman.2017.08.082)

45. Kanoğlu, M., Çengel, Y. A., & Dinçer, İ. (2012). Efficiency evaluation of energy systems. Springer Science & Business Media.

46. Medica-Viola, V., Mrzljak, V., Anđelić, N., & Jelić, M. (2020). Analysis of Low-Power Steam Turbine With One Extraction for Marine Applications. NAŠE MORE: znanstveni časopis za more i pomorstvo, 67(2), 87-95. (doi:10.17818/NM/2020/2.1)

47. Kocijel, L., Poljak, I., Mrzljak, V., & Car, Z. (2020). Energy loss analysis at the gland seals of a marine turbo-generator steam turbine. Tehnički glasnik, 14(1), 19-26. (doi:10.31803/tg-20191031094436)

48. Mrzljak, V., & Poljak, I. (2019). Energy analysis of main propulsion steam turbine from conventional LNG carrier at three different loads. NAŠE MORE: znanstveni časopis za more i pomorstvo, 66(1), 10-18. (doi:10.17818/NM/2019/1.2)

49. Aljundi, I. H. (2009). Energy and exergy analysis of a steam power plant in Jordan. Applied thermal engineering, 29(2-3), 324-328. (doi:10.1016/j.applthermaleng.2008.02.029)

50. Mrzljak, V., Poljak, I., & Žarković, B. (2018). Exergy analysis of steam pressure reduction valve in marine propulsion plant on conventional LNG carrier. NAŠE MORE: znanstveni časopis za more i pomorstvo, 65(1), 24-31. (doi:10.17818/NM/2018/1.4)

51. Wu, J., & Wang, N. (2020). Exploring avoidable carbon emissions by reducing exergy destruction based on advanced exergy analysis: A case study. Energy, 206, 118246. (doi:10.1016/j.energy.2020.118246)

52. Mrzljak, V., Prpić-Oršić, J., & Poljak, I. (2018). Energy power losses and efficiency of low power steam turbine for the main feed water pump drive in the marine steam propulsion system. Pomorski zbornik, 54(1), 37-51. (doi:10.18048/2018.54.03)

53. Baldi, F., Ahlgren, F., Nguyen, T. V., Thern, M., & Andersson, K. (2018). Energy and exergy analysis of a cruise ship. Energies, 11(10), 2508. (doi:10.3390/en11102508)

54. Mrzljak, V., Poljak, I., & Prpić-Oršić, J. (2019). Exergy analysis of the main propulsion steam turbine from marine propulsion plant. Brodogradnja: Teorija i praksa brodogradnje i pomorske tehnike, 70(1), 59-77. (doi:10.21278/brod70105)

55. Ogorure, O. J., Oko, C. O. C., Diemuodeke, E. O., & Owebor, K. (2018). Energy, exergy, environmental and economic analysis of an agricultural waste-to-energy integrated multigeneration thermal power plant. Energy conversion and management, 171, 222-240. (doi:10.1016/j.enconman.2018.05.093)

56. Mrzljak, V., Prpić-Oršić, J., & Senčić, T. (2018). Change in steam generators main and auxiliary energy flow streams during the load increase of LNG carrier steam propulsion system. Pomorstvo, 32(1), 121-131. (doi:10.31217/p.32.1.15)

57. Dincer, I., & Rosen, M. A. (2012). Exergy: energy, environment and sustainable development. Newnes.

58. Mrzljak, V., Senčić, T., & Žarković, B. (2018). Turbogenerator steam turbine variation in developed power: Analysis of exergy efficiency and exergy destruction change. Modelling and Simulation in Engineering, 2018. (doi:10.1155/2018/2945325)

59. Mrzljak, V., Kudláček, J., Begić-Hajdarević, Đ., & Musulin, J. (2020). The Leakage of Steam Mass Flow Rate through the Gland Seals–Influence on Turbine Produced Power. Pomorski zbornik, 58(1), 39-56. (doi:10.18048/2020.58.03.)

60. Elhelw, M., Al Dahma, K. S., & el Hamid Attia, A. (2019). Utilizing exergy analysis in studying the performance of steam power plant at two different operation mode. Applied Thermal Engineering, 150, 285-293. (doi:10.1016/j.applthermaleng.2019.01.003)

61. Lorencin, I., Anđelić, N., Mrzljak, V., & Car, Z. (2019). Exergy analysis of marine steam turbine labyrinth (gland) seals. Pomorstvo, 33(1), 76-83. (doi:10.31217/p.33.1.8)

62. Mrzljak, V. (2018). Low power steam turbine energy efficiency and losses during the developed power variation. Tehnički glasnik, 12(3), 174-180. (doi:10.31803/tg-20180201002943)

63. Tan, H., Shan, S., Nie, Y., & Zhao, Q. (2018). A new boil-off gas re-liquefaction system for LNG carriers based on dual mixed refrigerant cycle. Cryogenics, 92, 84-92. (doi:10.1016/j.cryogenics.2018.04.009)

64. Moran, M. J., Shapiro, H. N., Boettner, D. D., & Bailey, M. B. (2010). Fundamentals of engineering thermodynamics. John Wiley & Sons.

65. Erdem, H. H., Akkaya, A. V., Cetin, B., Dagdas, A., Sevilgen, S. H., Sahin, B., ... & Atas, S. (2009). Comparative energetic and exergetic performance analyses for coal-fired thermal power plants in Turkey. International Journal of Thermal Sciences, 48(11), 2179-2186. (doi:10.1016/j.ijthermalsci.2009.03.007)

66. Noroozian, A., Mohammadi, A., Bidi, M., & Ahmadi, M. H. (2017). Energy, exergy and economic analyses of a novel system to recover waste heat and water in steam power plants. Energy conversion and management, 144, 351-360. (doi:10.1016/j.enconman.2017.04.067)

67. Blažević, S., Mrzljak, V., Anđelić, N., & Car, Z. (2019). Comparison of energy flow stream and isentropic method for steam turbine energy analysis. Acta Polytechnica, 59(2), 109-125. (doi:10.14311/AP.2019.59.0109)

68. Ray, T. K., Datta, A., Gupta, A., & Ganguly, R. (2010). Exergy-based performance analysis for proper O&M decisions in a steam power plant. Energy Conversion and Management, 51(6), 1333-1344. (doi:10.1016/j.enconman.2010.01.012)

69. Mrzljak, V., Poljak, I., & Mrakovčić, T. (2017). Energy and exergy analysis of the turbo-generators and steam turbine for the main feed water pump drive on LNG carrier. Energy conversion and management, 140, 307-323. (doi:10.1016/j.enconman.2017.03.007)

70. Eboh, F. C., Ahlström, P., & Richards, T. (2017). Exergy analysis of solid fuel-fired heat and power plants: a review. Energies, 10(2), 165. (doi:10.3390/en10020165)

71. Uysal, C., Kurt, H., & Kwak, H. Y. (2017). Exergetic and thermoeconomic analyses of a coal-fired power plant. International Journal of Thermal Sciences, 117, 106-120. (doi:10.1016/j.ijthermalsci.2017.03.010)

72. Kakac, S., Liu, H., & Pramuanjaroenkij, A. (2020). Heat exchangers: selection, rating, and thermal design. CRC press.

73. Annaratone, D. (2010). Handbook for Heat exchangers and tube Banks design. Springer Science & Business Media.

74. Lemmon, E. W., Huber, M. L., & McLinden, M. O. (2010). NIST Standard Reference Database 23, Reference Fluid Thermodynamic and Transport Properties (REFPROP), version 9.0, National Institute of Standards and Technology. R1234yf. fld file dated December, 22, 2010.

75. Taheri, M. H., Mosaffa, A. H., & Farshi, L. G. (2017). Energy, exergy and economic assessments

of a novel integrated biomass based multigeneration energy system with hydrogen production and LNG regasification cycle. Energy, 125, 162-177. (doi:10.1016/j.energy.2017.02.124)

76. Mrzljak, V., Žarković, B., & Poljak, I. (2017). Energy and exergy analysis of sea water pump for the main condenser cooling in the LNG carrier steam propulsion system. Mathematical Modeling, 1(3), 144-147.

77. Saravanamuttoo, H. I., Rogers, G. F. C., & Cohen, H. (2001). Gas turbine theory. Pearson Education.

78. Kostyuk, A., & Frolov, V. (1988). Steam and gas turbines. Mir Publishers.

79. Malik, A., Zheng, Q., & Lin, A. (2019). The design and performance analysis of highly loaded compressor of closed Brayton cycle HTGR power plant with helium xenon gas mixture as working fluid. Progress in Nuclear Energy, 117, 103084. (doi:10.1016/j.pnucene.2019.103084)

80. Bammert, K., Krey, G., & Krapp, R. (1974, April). Operation and Control of the 50-MW Closed-Cycle Helium Turbine Oberhausen. In ASME 1974 International Gas Turbine Conference and Products Show. American Society of Mechanical Engineers Digital Collection. (doi:10.1115/74-GT-13)

81. Hafdhi, F., Khir, T., Yahyia, A. B., & Brahim, A. B. (2015). Energetic and exergetic analysis of a steam turbine power plant in an existing phosphoric acid factory. Energy Conversion and Management, 106, 1230-1241. (doi:10.1016/j.enconman.2015.10.044)

82. Kopac, M., & Hilalci, A. (2007). Effect of ambient temperature on the efficiency of the regenerative and reheat Çatalağzı power plant in Turkey. Applied Thermal Engineering, 27(8-9), 1377-1385. (doi:10.1016/j.applthermaleng.2006.10.029)

83. Glavan, I., & Prelec, Z. (2012). The analysis of trigeneration energy systems and selection of the best option based on criteria of GHG emission, cost and efficiency. Engineering Review, 32(3), 131-139.

84. Glavan, I., Prelec, Z., & Pavkovic, B. (2015). Modelling, simulation and optimization of small-scale CCHP energy systems. International Journal of Simulation Modelling, 14(4), 683-696. (doi:10.2507/IJSIMM14(4)10.336)

85. Baressi Šegota, S., Anđelić, N., Kudláček, J., & Čep, R. (2019). Artificial neural network for predicting values of residuary resistance per unit weight of displacement. Pomorski zbornik, 57(1), 9-22. (doi:10.18048/2019.57.01.)

86. Baressi Šegota, S., Lorencin, I., Ohkura, K., & Car, Z. (2019). On the traveling salesman problem in nautical environments: an evolutionary computing approach to optimization of tourist route paths in Medulin, Croatia. Pomorski zbornik, 57(1), 71-87. (doi:10.18048/2019.57.05.)

87. Lorencin, I., Anđelić, N., Mrzljak, V., & Car, Z. (2019). Genetic Algorithm Approach to Design of Multi-Layer Perceptron for Combined Cycle Power Plant Electrical Power Output Estimation. Energies, 12(22), 4352. (doi:10.3390/en12224352)

88. Lorencin, I., Anđelić, N., Španjol, J., & Car, Z. (2020). Using multi-layer perceptron with Laplacian edge detector for bladder cancer diagnosis. Artificial Intelligence in Medicine, 102, 101746. (doi:10.1016/j.artmed.2019.101746)

89. Lorencin, I., Anđelić, N., Šegota, S. B., Musulin, J., Štifanić, D., Mrzljak, V., ... & Car, Z. (2021). Edge Detector-Based Hybrid Artificial Neural Network Models for Urinary Bladder Cancer Diagnosis. In Enabling AI Applications in Data Science (pp. 225-245). Springer, Cham.

90. Baressi Šegota, S., Anđelić, N., Lorencin, I., Saga, M., & Car, Z. (2020). Path planning optimization of six-degree-of-freedom robotic manipulators using evolutionary algorithms. International Journal of Advanced Robotic Systems, 17(2), 1729881420908076. (doi:10.1177/1729881420908076)

91. Anđelić, N., Baressi Šegota, S., Lorencin, I., Jurilj, Z., Šušteršič, T., Blagojević, A., ... & Car, Z. (2021). Estimation of COVID-19 Epidemiology Curve of the United States Using Genetic Programming Algorithm. International Journal of Environmental Research and Public Health, 18(3), 959. (doi:10.3390/ijerph18030959)

92. Car, Z., Baressi Šegota, S., Anđelić, N., Lorencin, I., & Mrzljak, V. (2020). Modeling the Spread of COVID-19 Infection Using a Multilayer Perceptron. Computational and Mathematical Methods in Medicine, 2020. (doi:10.1155/2020/5714714)

93. Anđelić, N., Baressi Šegota, S., Lorencin, I., Mrzljak, V., & Car, Z. (2021). Estimation of COVID-19 epidemic curves using genetic programming algorithm. Health Informatics Journal, 27(1), 1460458220976728. (doi:10.1177/1460458220976728)